

Brain mechanisms of arithmetic: a crucial role for ventral temporal cortex

Journal:	<i>Journal of Cognitive Neuroscience</i>
Manuscript ID	JOCN-2018-0029.R1
Manuscript Type:	Original
Date Submitted by the Author:	17-May-2018
Complete List of Authors:	Pinheiro-Chagas, Pedro; Université Paris-Sud, Université Paris-Saclay Daitch, Amy; Stanford University Medical Center Parvizi, Josef; Stanford University Department of Neurology and Neurological Sciences Dehaene, Stanislas; INSERM CEA Cognitive Neuroimaging Unit
Keywords:	mental arithmetic, problem-size effect, ventral temporal cortex, intraparietal sulcus, intracranial electroencephalography

Title: **Brain mechanisms of arithmetic: a crucial role for ventral temporal cortex**
Running title: **Mental arithmetic in the ventral temporal cortex**

Pedro Pinheiro-Chagas^{1,*}, Amy Daitch^{2,*}, Josef Parvizi² and Stanislas Dehaene^{1,3}

1. Cognitive Neuroimaging Unit, CEA DRF/I2BM, INSERM, Université Paris-Sud, Université Paris-Saclay, NeuroSpin center, 91191 Gif/Yvette, France
2. Laboratory of Behavioral and Cognitive Neuroscience, Stanford Human Intracranial Cognitive Electrophysiology Program, Department of Neurology and Neurological Sciences, Stanford University, Stanford, CA 94305
3. Collège de France, 11 Place Marcelin Berthelot, 75005 Paris, France
* These authors contributed equally to this work

Corresponding author:
Pedro Pinheiro-Chagas
ppinheirochagas@gmail.com
Cognitive Neuroimaging Unit
DRF/JOLIOT/NEUROSPIN/UNICOG
Bât. 145 - Point Courrier 156
F-91191 GIF SUR YVETTE Cedex FRANCE

Acknowledgments:
We thank all the patients for volunteering their time to participate in this study; members of the Laboratory of Behavioral and Cognitive Neuroscience at Stanford University for their help in the initial and early stages of this study. This work was supported by research Grant R01NS078396 from the National Institute of Neurological Disorders, Stroke; Grant 1R01MH109954-01 from the National Institute of Mental Health (NIMH), Grant BCS1358907 from the National Science Foundation (NSF) (all to J.P.) and by the INSERM, CEA, and the Bettencourt-Schueller Foundation (France). Postdoctoral Fellowship 1F32HD087028-01 from the National Institute of Child Health and Human Development (to A.L.D.); Science Without Borders Fellowship from CNPq – Brazil (nr. 246750/2012-0). The views presented in this work do not necessarily reflect those of the National Institutes of Health. The authors declare no conflicts of interest.

Abstract

Elementary arithmetic requires a complex interplay between several brain regions. The classical view, arising from functional magnetic resonance imaging (fMRI), is that the intraparietal sulcus (IPS) and the superior parietal lobe (SPL) are the main hubs for arithmetic calculations. However, recent studies using intracranial electroencephalography (iEEG) have discovered a specific site, within the posterior inferior temporal cortex (pITG), that activates during visual perception of numerals, with widespread adjacent responses when numerals are used in calculation. Here, we re-examined the contribution of the IPS, SPL and pITG to arithmetic by recording iEEG signals while subjects solved addition problems. Behavioral results showed a classical problem-size effect: RTs increased with the size of the operands. We then examined how high-frequency broadband (HFB) activity is modulated by problem size. As expected from previous fMRI findings, we showed that the total high-frequency broadband (HFB) activity in IPS and SPL site increased with problem size. More surprisingly, pITG sites showed an initial burst of HFB activity that decreased as the operands got larger, yet with a constant integral over the whole trial, thus making these signals invisible to slow fMRI. While parietal sites appear to have a more sustained function in arithmetic computations, the pITG may have a role of early identification of the problem difficulty, beyond merely digit recognition. Our results ask for a re-evaluation of the current models of numerical cognition and reveal that the ventral temporal cortex contains regions specifically engaged in mathematical processing.

1
2
3
4
5
6
7
8
9
10
11
12
13
14
15
16
17
18
19
20
21
22
23
24
25
26
27
28
29
30
31
32
33
34
35
36
37
38
39
40
41
42
43
44
45
46
47
48
49
50
51
52
53
54
55
56
57
58
59
60

23 **Key words:** mental arithmetic, electrocorticography, problem-size effect, ventral
24 temporal cortex, intraparietal sulcus

For Review Only

25 Introduction

26 Elementary arithmetic requires a complex interplay between several brain
27 regions. The classical Triple-Code model for numerical cognition proposed that the
28 lateral parietal cortex (LPC) hosts the main hubs for numerosity representation and
29 manipulation (Dehaene, Piazza, Pinel, & Cohen, 2003; Piazza, Izard, Pinel, Le Bihan, &
30 Dehaene, 2004; Piazza, Pinel, Le Bihan, & Dehaene, 2007; Pinel, Dehaene, Rivie, &
31 Lebihan, 2001). Indeed, convergent brain-imaging, intracranial recording and
32 stimulation studies have found that the intraparietal sulcus (IPS) is selectively activated
33 (Menon, Rivera, White, Glover, & Reiss, 2000; Stanescu-Cosson et al., 2000) and
34 causally involved in mental arithmetic (Della Puppa et al., 2013; Semenza, Salillas, De
35 Pallegirin, & Della Puppa, 2017). Furthermore, IPS activity has also been shown to
36 increase as problems become harder (De Smedt, Holloway, & Ansari, 2011; Dehaene,
37 Spelke, Pinel, Stanescu, & Tsivkin, 1999; Kanjlia, Lane, Feigenson, & Bedny, 2016;
38 Molko et al., 2003; Visscher et al., 2015), thus paralleling the classical behavioral
39 problem-size effect, which is an increase in calculation time as a function of the
40 magnitude of the operands (Ashcraft, 1992). Moreover, the superior parietal lobe (SPL)
41 is also activated during calculation (Knops, Thirion, Hubbard, Michel, & Dehaene, 2009),
42 and recent studies have reported that it hosts a topographic map of numerosity (Harvey,
43 Klein, Petridou, & Dumoulin, 2013; Harvey, Ferri, & Orban, 2017).

44 In addition to the LPC, the Triple-Code model predicted that the ventral temporal
45 cortex (VTC) would have a key role in number recognition. Indeed, recent studies using
46 intracranial electroencephalography (iEEG) have confirmed the existence of a region in
47 the posterior inferior temporal gyrus (pITG) that selectively activates during visual

1
2
3 48 identification of Arabic numerals (the ‘number form area’, NFA), as compared to other
4
5 49 similar morphometric symbols, such as letters (Shum et al., 2013). Subsequent iEEG
6
7 50 studies have demonstrated that distinct neuronal populations adjacent to the NFA, also
8
9 51 within the pITG, respond higher (Hermes et al., 2015) or exclusively (Daitch et al., 2016)
10
11 52 to numerals when they are in the context of a calculation and that these pITG sites have
12
13 53 high functional connectivity with the IPS (Daitch et al., 2016). These results raised the
14
15 54 possibility that pITG might be involved in arithmetic processing beyond visual
16
17 55 recognition of mathematical symbols, which is unexpected from previous fMRI and
18
19 56 neuropsychological findings, unpredicted by neurocognitive models of arithmetic, and
20
21 57 surprising given the traditional view of the VTC as the last stage of the ventral “what”
22
23 58 visual pathway, associated with object categorization (Grill-Spector & Weiner, 2014).
24
25 59 However, these prior studies that investigated the role of pITG in arithmetic processing
26
27 60 were restricted to either contrasts between numerals and similar morphometric symbols
28
29 61 or between calculation and other tasks (e.g., memory/sentence comprehension), thus
30
31 62 never testing if, how and when the activity in pITG is modulated by numerical features of
32
33 63 calculations. Consequently, the precise role of pITG in mathematical cognition remains
34
35 64 largely elusive.

36
37
38
39
40
41
42 65 In the present study, we aimed at re-evaluating the roles of IPS, SPL and pITG in
43
44 66 mental calculation with an unprecedented level of precision, by recording
45
46 67 electrophysiological signals directly from the human cortex (iEEG). We asked subjects
47
48 68 to verify the correctness of visually presented additions, in the form of “13+5=17”, in
49
50 69 which we systematically varied the size of the problems (i.e., magnitude of the
51
52
53
54
55
56
57
58
59
60

operands), while preserving the same structure and number of characters, thus separating numerical from low-level visual features of the stimuli.

Based on previous fMRI findings, we predicted that the overall activity in the IPS and SPL would be sustained and increase as a function of problem-size. Furthermore, this parametric modulation should be correlated with RT. However, we were less certain about the pITG. If it is only involved in the visual recognition of numerals, we should expect a brief transient burst of activity with no parametric modulation by problem-size. But, since multi-digit calculations might require subjects to mentally re-evaluate the problem a few times before they reach a final decision, pITG activity may be sustained across the trial and increase as a function of problem-size, possibly reflecting the top-down attentional modulation from LPC. Finally, the pITG could be parametrically modulated by problem-size, but in a different way and with a different latency as compared to IPS and SPL, thus revealing an unpredicted role in calculation.

Materials and Methods

Subjects

We recorded electrocorticography data from 10 patients with epilepsy who were implanted with intracranial electrodes over the VTC and/or LPC as part of their pre-surgical evaluation at Stanford University Medical Center. Demographic information for each subject is included in Table 2. Each subject was monitored in the hospital for approximately 6-10 days following surgery, during which they participated in our study. Before participating, all subjects provided verbal and written consent, which was approved by the Stanford Institutional Review Board. Part of the data of the present

cohort was already published elsewhere (Daitch et al., 2016; Hermes et al., 2015; Shum et al., 2013). The inclusion criterion in this study was the completion of at least 80 trials (corresponding to two blocks) of the Arithmetic condition, to have enough power to investigate parametric modulations within condition (see below).

Behavioral tasks

Arithmetic & Memory Verification: Subjects were asked to verify the correctness of either addition calculations (e.g., “13+5=17”, Arithmetic condition) or autobiographical memory statements (e.g., “I ate fruit yesterday”, Memory condition), visually presented and randomly intermixed within the same block. For the purposes of the present study, the “Memory condition” served as a sentence/language comprehension control condition for Arithmetic. Additions were always composed of a 2-digit operand (ranging from 10 to 87), a 1-digit operand (ranging from 1 to 9, excluding 3) in either order and a 2-digit proposed result (Table 1). In half of the trials, the proposed result was correct. The absolute deviant for the incorrect proposed results ranged from 1-16. Subjects responded in the self-paced manner, by pressing one of two keypad buttons. The trials were interspersed with fixation periods (5s or 10s), during which subjects were simply asked to fixate at a crosshair in the center of the screen. A 200 ms ITI separated trials. All subjects but one verified 80 additions and 50 memory statements (S1 evaluated 120 additions and 100 memory statements), divided in 2 blocks of 40 additions and 25 memory statements each.

[TABLE 1]

Symbol Identification: Subjects were visually presented with a series of symbols falling under one of three categories: (1) Arabic numerals (ranging from 1-9), (2) letters in the Latin alphabet (A, C, D, E, H, N, R, S, or T), or (3) letters in foreign alphabets. Each category had 72 trials randomly shuffled and divided in 2 blocks. For each symbol, subjects had to press a given button if they could read the symbol (i.e., numbers or letters in the Latin alphabet) and another button if they could not read it (i.e., symbols in foreign alphabets). Subjects had up to 15 s to respond to each stimulus and trials were separated by a 500-ms ITI. The tasks were presented on a laptop computer (Apple MacBook or MacBook Pro), using MATLAB's Psychtoolbox (Brainard, 1997).

Electrodes

Each subject was implanted with grids and/or strips of subdural platinum electrodes (AdTech Medical Instruments Corporation), whose locations were determined purely for clinical reasons. Each electrode had an exposed diameter of 2.3 mm, with inter-electrode spacing of 10mm, 7mm, or 5mm for higher density arrays.

Electrode localization. Electrode locations were mapped on each subject's own cortical surface with the following steps: 1) A post-surgical CT (with electrodes) was aligned to a pre-surgical T1-weighted MRI using SPM8 (<http://www.fil.ion.ucl.ac.uk/spm/>). 2) Electrode coordinates were manually localized within the aligned CT as the center of high image intensity spheres. 3) The identified electrode coordinates were adjusted for minor cortical shifts following surgery, with a local projection defined separately for each grid or strip (Hermes, Miller, Noordmans, Vansteensel, & Ramsey, 2010). 4) Cortical surface reconstructions of each subject's

brain were obtained by manually segmenting the white matter from the subject's T1-weighted MRI using ITKGray (<http://vistalab.stanford.edu/newlm/index.php/ItkGray>) and growing out 2 layers of grey matter from the white matter surface. Finally, electrodes were labeled by an expedient neuroanatomist, based on the subdivision of LPC and VTC showed in **Figure 1**. For group plots, each subject's electrode coordinates, defined in native brain space, were realigned to a normalized brain (MNI Colin 27 (<http://www.bic.mni.mcgill.ca/ServicesAtlases/Colin27>), and coordinates across subjects were plotted in this common space. Note that the location of each electrode site projected in MNI space may look slightly different (relative to gyral landmarks, etc) than in native space, and was done purely for visualization purposes. Anatomical parcellations within the VTC and LPC were determined based on each subject's own gyral landmarks in native brain space.

Data acquisition and analysis

iEEG data were recorded from subdural electrodes via a multichannel recording system (Tucker David Technologies). Data were acquired with a band pass filter of 0.5-300 Hz and sampling rate of 1525.88 Hz. An electrode outside the seizure zone with the most silent electrocorticographic activity was selected as an online reference during acquisition. **Preprocessing.** First, electrodes with epileptiform activity, or those corrupted by electrical noise, were eliminated from subsequent analyses. Electrodes were also excluded whose overall power was five or more standard deviations above or below the mean power across channels, and those whose power spectrum strayed from

the normal $1/f$ power spectrum, based on visual inspection. All non-excluded channels were then notch filtered at 60 Hz and harmonics to remove electric interference, then re-referenced to the mean of the filtered signals of the non-excluded channels. The re-referenced signal at each electrode was then band-pass filtered between 70 and 180 Hz (high frequency broadband, HFB) using sequential 10 Hz width band-pass windows (70-80 Hz, 80-90 Hz, etc.), using two-way, zero-lag, FIR filters. The instantaneous amplitude of each band-limited signal was computed by taking the modulus of the Hilbert Transformed signal. The amplitude of each 10 Hz band signal was normalized by its own mean, then these normalized amplitude time series were averaged together, yielding a single amplitude time-course for the HFB band.

Task-related HFB changes

Our analyses were focused on task-induced changes in HFB activity (70-180 Hz), due to its high correlation with local spiking activity and the fMRI BOLD signal (Foster, Rangarajan, Shirer, & Parvizi, 2015; Logothetis, Pauls, Augath, Trinath, & Oeltermann, 2001; Manning, Jacobs, Fried, & Kahana, 2009; Parvizi et al., 2012; Ray & Maunsell, 2011). For the **Arithmetic & Memory verification task**, we first identified electrodes within the VTC and LPC that responded selectively during arithmetic calculations relative to reading sentences comprehension/memory retrieval. We classified all sites into six groups based on their relative responses during arithmetic vs. memory trials. 1) **Arithmetic active** channels were defined as those with significantly greater HFB activity during arithmetic trials (0 - 1,000 ms following stimulus onset) than during baseline (200 ms inter-trial interval); 2) **Arithmetic selective** channels satisfied 1, and also exhibited

significantly greater HFB activity during arithmetic than memory trials (0 - 1,000 ms following stimulus onset for each condition); 3) **Arithmetic-only** channels satisfied 1 and 2, and additionally exhibited no significant increase in activity during memory trials (0 - 1,000 ms following stimulus onset). 4-6) **Memory-active, memory-selective, and memory-only** channels were classified using equivalent criteria as 1-3, but comparing activity during memory trials to that during baseline or arithmetic trials. For the **Symbol identification task**, a similar procedure was used to determine channel selectivity, but using a time-window of (0 – 400 ms after stimuli onset) and a baseline of (-200 ms before stimuli onset). Channels were classified as 1) **Numeral active** if they showed significantly greater HFB activity during numerals identification as compared to baseline; 2) **Numeral selective** channels satisfied 1 and also exhibited significantly greater HFB activity during numerals identification as compared to Latin and foreign letters. Unpaired permutation tests were run to test for differences in HFB power between different task conditions, while paired permutation tests were run to test for a difference in HFB power between a task condition and baseline. All p-values in all analyses were FDR corrected by the total number of VTC and LPC channels within each subject.

Results

Behavior results

Accuracy for the Arithmetic condition was high (80% or higher) in 9/10 subjects (Table 2). To model RTs in each subject, we calculated stepwise regression models with the smaller operand (*min*), the larger operand (*max*), the sum and the absolute deviant as predictors. Results revealed that the *min* operand was a significant and the

best predictor of RT in 9/10 subjects ($\text{betas} > 0.32$, $p < 0.003$), while the sum and the absolute deviant were significant predictors only in 2 subjects ($\text{betas} > 0.28$, $p < 0.01$). The *max* operand was not a significant predictor of RT in any model (Table 3).

[TABLE 2]

These behavioral results corroborate previous findings using a variety of paradigms, such as verification (Groen & Parkman, 1972), production (Barrouillet & Thevenot, 2013; Uittenhove, Thevenot, & Barrouillet, 2016) and number-to-position (Pinheiro-Chagas, Dotan, Piazza, & Dehaene, 2017) in which the *min* operand was also found to be the best predictor of RT (Barrouillet & Thevenot, 2013; Groen & Parkman, 1972; Pinheiro-Chagas et al., 2017; Uittenhove et al., 2016), thus providing convergent evidence that the *min* operand is a robust and reproducible index of problem-size/difficulty.

[TABLE 3]

Selectivity for Arithmetic in pITG, aIPS and SPL sites

Next, we investigated the Arithmetic vs. Memory selectivity in several recording sites across all subjects. We found that our Arithmetic-ROIs - pITG, aIPS, and SPL - were highly selective to arithmetic processing, as previously reported (Daitch et al., 2016; Hermes et al., 2015) and in line with a recent fMRI study that used an analogous task (Amalric & Dehaene, 2016). 40% of sites within the pITG (11/28), 21% of sites around the aIPS (7/33) and 25% of sites within the SPL (13/53) responded exclusively during the arithmetic condition (Figure 1C). Moreover, most of the arithmetic-selective

sites in these regions exhibited sustained activity during the computation. In sharp contrast, the Memory condition produced activity in the language network including LPC regions such as the angular gyrus and superior temporal sulcus (Pallier, Devauchelle, & Dehaene, 2010) and in more medial portions of the inferior temporal cortex, close to the visual word form area (VWFA, Hannagan, Amedi, Cohen, Dehaene-Lambertz, & Dehaene, 2015). Non-selective sites, showed either transient activity following stimulus onset in both conditions, likely involved in the visual processing of the stimulus, or later activity just prior to subjects' motor response, probably engaged in motor planning.

[FIGURE 1]

Parametric modulation of HFB power by *min* operand in pITG, aIPS and SPL

Given the behavioral evidence that the *min* operand was the best index of problem size/difficulty, we next investigated if, how and when the *min* operand modulated the activity in our Arithmetic-ROIs. To do so, we performed linear regression analysis on the HFB activity at each recording site on two time windows: *initial activity* (averaged power over 0 - 1,000 ms following stimulus onset, where greater activity was observed) and *total activity* (the integral - area under the curve - from stimulus onset to subject's RT)

[TABLE 4]

As expected from previous fMRI findings, the *total activity* increased as a function of *min* operand in several aIPS (5/12 sites, 42% in 3/7 subjects with aIPS coverage) and SPL (7/17 sites, 41% in 3/7 subjects with SPL coverage) sites ($p < 0.05$, FDR corrected; Table 4, Figures 2a, 3 and 5a). Importantly, no site in pITG showed this effect.

Surprisingly, however, we found that the *initial activity* significantly decreased as a function of *min* operand ($p < 0.05$, FDR corrected) in several arithmetic-selective pITG sites (10/17, 59% in 6/7 subjects with pITG coverage) and in 1 anterior ITG site, just adjacent to the pITG (Table 4). Examples of activation profiles at the single trial level are shown in Figure 2b (see also Figures 4 and 5a). This proportion increased when considering only the arithmetic-selective channels that did not show any significant response during the memory condition (arithmetic-only channels: 8/11, 72%).

The same effect was also observed in a small proportion of the arithmetic-selective channels in the aIPS and SPL (aIPS: 2/12, 17% in 2/7 subjects with aIPS coverage; SPL: 2/17 sites, 12% in 2/7 subjects with SPL coverage). But as can be seen in Figure 5a, the pattern of modulation by problem-size/difficulty is overall highly dissociable between and arithmetic selective ITG in aIPS/SPL sites. Indeed, the effect of *min* operand in the initial activity was much higher (negative sign) for the ITG sites that showed a significant decrease in the initial activity as compared to the aIPS/SPL sites that showed a significant increase in total activity (mean beta in ITG = -0.3828 , $sd = 0.0619$; mean beta aIPS/SPL = -0.104 , $sd = 0.143$; $t(21) = -5.932$, $p < 0.001$). Conversely, the effect of *min* operand in the total activity was much higher for the aIPS/SPL sites that showed a significant increase in the total activity as compared to the ITG sites that showed a significant decrease in the initial activity (mean beta in

aIPS/SPL = 0.422, sd = 0.077; mean beta aIPS/SPL = -0.056, sd = 0.1538; $t(21) = 9.562$, $p < 0.001$).

[FIGURE 2]

[FIGURE 3]

[FIGURE 4]

To evaluate the specificity of these results, we next analyzed functional control sites, where activity was memory-selective or equally responsive to arithmetic and memory (Table 5), as well as anatomical control sites (arithmetic-selective channels that were outside of our Arithmetic-ROIs, Table 6). None of the memory selective channels, nor channels that equally responded to arithmetic and memory, across any brain region, showed a significant decrease in the initial HFB activity as a function of *min* operand. Very few non-arithmetic-selective channels in the ROIs showed an increase of total HFB activity as a function of *min* operand.

[TABLE 5]

Likewise, very few arithmetic selective channels located outside the ROIs showed either a decrease in the initial HFB activity or an increase in the total HFB activity as a function of *min* operand.

[TABLE 6]

In summary, parametric modulations were almost entirely dissociated into two categories, found in both left and right hemispheres (Figure 5): (1) decreases in *initial activity* with increasing *min* operand, showing a high specificity to arithmetic-selective sites mostly in pITG, and (2) increases in *total activity* with increasing *min* operand in aIPS and SPL arithmetic selective sites.

Specificity of the pITG modulation to calculation

Was the pITG modulation due to calculation itself? An alternative possibility is that this is a visual recognition effect. The smaller a numeral is, the higher is its frequency in spoken and written language (Dehaene & Mehler). Thus, visual frequency (greater activation to frequent digits) rather than calculation difficulty could drive the pITG effect. However, this would predict that the effect should be found whenever subjects process digits, even in the absence of any calculation.

In order to test whether the modulation observed in the pITG by the magnitude of the min operand was present in any context or exclusively during arithmetic calculations, we analyzed the data of the Symbol Identification task. First, we investigated the selectivity to symbols in the ITG sites that showed decreased activity as a function of min operand. We found that 7/11 sites were active, but not selective to Arabic numerals, that is, they equally responded to Latin and foreign letters (Table 7). And the remaining 4 sites were not even active for any symbol. Only one site showed selectivity for numerals, thus qualifying for belonging to the 'number form area' (NFA; {ref}). Those findings fit with recent evidence that the NFA occupies a small ventral occipito-temporal

site, and that many more lateral sites respond to calculation itself rather than mere digit recognition (Daitch et al., 2016; Grotheer, Jeska, & Grill-Spector, 2018).

Next, we performed a linear regression analysis on the averaged HFB power during symbol identification, between 0 – 500 ms, the window where the highest activity was observed, with the Arabic numerals (ranging from 1-9) as predictors. None of the 11 sites showed a significant positive or negative effect of number magnitude ($p > 0.1$, FDR corrected for only the 11 channels, to be more liberal). Therefore, the engagement and selectivity to mathematical objects/processing in the ITG was much more selective during calculation as compared to digit recognition and, crucially, the parametric modulation by number magnitude (*min operand*) was exclusively present during calculation.

[TABLE 7]

Other potential confounds

The list of arithmetic problems used in our study were not constructed with the problem-size effect in mind, and the *min* variable may therefore be confounded with other variables. In particular, we thank one of the anonymous reviewers for spotting that 'number of unique digits' had a small positive correlation with *min operand* ($\rho = 0.23$, $p = 0.041$) (e.g. $10 + 1 = 11$ has 2 unique digits, while $47 + 9 = 56$ has 5). If the ITG sites were purely engaged in digit recognition, their activity could be more lower for trials with fewer distinct digits, thus potentially explaining the *min* effect. To evaluate this possibility, we used a multiple regression approach. First, we excluded trials with only 2 unique digits, since they were only present in problems with *min operand* = 1. This already

reduced the correlation between NUD and *min* operand to $\rho = 0.20$, $p = 0.08$. Next, we ran a multiple regression model with *min* operand and NUD as predictors. The effect of the *min* operand clearly dominated: it remained significant in 9/11 ITG sites ($p < 0.05$, FDR corrected). Crucially, the 'number of unique digits' did not significantly explain unique variance in any of the ITG sites ($p > 0.6$, FDR corrected). Therefore, we can clearly refute this possible confound.

The absolute distance between the proposed result and the correct result also had a small, non-significant negative correlation with *min* operand ($\rho = -0.17$, $p = 0.113$) and is known to affect arithmetic verification {refs}. To evaluate whether the observed ITG modulation originated from a distance effect at the verification stage, we again ran a multiple regression model with *min* operand and *absolute deviant* as predictors. Once again, the effect of *min* operand clearly dominated: it was unaffected in all 11 ITG sites ($p < 0.05$, FDR corrected). Crucially, the *absolute distance* did not significantly explain unique variance at any of the ITG sites ($p > 0.5$, FDR corrected).

A third variable that is known to affect calculation (Ashcraft, 1992) and was necessarily confounded with the size of the *min* operand is decade crossing, i.e. whether the addition crosses a decade boundary such that the decade of the result is different from the decade of the first operand (e.g. $34+8=42$). In the present study, it is not trivial to completely disambiguate those two effects, the multiple regression suffers from multicollinearity, but we tested anyways. In the model with both *min* operand and decade crossing as predictors, the effect of *min* operand remained significant in 4/11 channels in pITG ($p < 0.01$). Importantly, decade crossing did not significantly explain unique variance in any of the ITG sites ($p > 0.3$) and the betas were overall much more

negative (stronger effect) for *min* operand as compared to decade crossing (mean *min* operand = -0.385, sd = 0.138; mean decade crossing = -0.001, sd = 0.185, $t(20) = -5.4840$, $p < 0.000$).

In summary, those control analyses suggest that the modulation observed in the pITG is indeed due to arithmetic problem-size/difficulty, which is primarily driven by the magnitude of the *min* operand. The design of the stimuli did not allow us to fully decorrelate the *min* operand from the *decade crossing* effect, and both variables may have contributed to problem difficulty, but the *min* effect seemed to be dominant.

Dissociation from reaction time

Finally, to verify if the parametric modulation by *min* operand directly translated to behavior, and whether this effect was independent of other factors that influence RT, such as attention, decision-making and motor preparation, we used multiple linear regression to model HFB activity as a function of both *min* operand and RT (Figure 5b and c). When regressing out the effect of RT, the *initial activity* at most pITG sites remained significantly modulated by *min* operand at 9 of the 10 observed sites. Conversely, once we regressed out the effect of RT from the *total activity* in aIPS and SPL, the effect of *min* operand completely vanished in all sites (Figure 5b). As shown in Figure 5c, the *total activity* in almost all VTC and LPC sites significantly correlated with RT, independently of *min* operand. Therefore, in contrast with the increase in *total activity* as a function of *min* operand observed in aIPS and SPL sites which proved to be directly related behavior, the parametric decrease of the *initial activity* as a function of *min* operand observed in pITG was partially dissociated from RT, possibly indicating a

role in the earlier stages of the calculation that does not directly translate into subsequent stages.

[FIGURE 5]

Discussion

By recording electrophysiological signals directly from the human cortex with remarkable temporal and spatial resolution, we characterized the response selectivity and parametric modulation patterns in neuronal populations of the lateral parietal and ventral temporal cortices during mental arithmetic. Our results demonstrated a high degree of selectivity for calculations in a network comprised of the aIPS and SPL in the LPC and the pITG in the VTC, almost completely dissociated from the selectivity observed during sentence comprehension (Memory condition), observed in the angular gyrus and STS and the medial inferior temporal cortex, known to be involved in language comprehension (Pallier et al., 2010) and reading (Hannagan, Amedi, Cohen, Dehaene-Lambertz, & Dehaene, 2015), respectively. This dissociation in line with previous reported iEEG results (Daich et al., 2016; Hermes et al., 2015), with a recent fMRI study that used an analogous task (Amalric & Dehaene, 2016), with a series of prior fMRI findings (Arsalidou & Taylor, 2011) and with studies that used intraoperative electrical stimulation (Della Puppa et al., 2013; Semenza et al., 2017).

All subjects performed the addition task with high accuracy, and their RT patterns reflected the most widely replicated behavioral effect in cognitive arithmetic: the

problem-size effect (Ashcraft, 1992; Zbrodoff & Logan, 2005). More specifically, we found that the best predictor of RT, and therefore problem size/difficulty, was the smaller of the two operands (called *min*), corroborating several studies which used a variety of paradigms, such as production, verification and number-to-position (Barrouillet & Thevenot, 2013; Groen & Parkman, 1972; Pinheiro-Chagas et al., 2017; Uittenhove et al., 2016). This result is also compatible with the original *Min Model* (Groen and Parkman, 1972) and with its recent variants, including the concept of "fast automated procedures" for scrolling on an ordered representation (Barrouillet & Thevenot, 2013; Uittenhove et al., 2016), or the hypothesis of a stepwise displacement on the "mental number line", starting with the max operand and incrementally adding the min operand (Pinheiro-Chagas et al., 2017). Nevertheless, the present results should not be seen as providing definitive support for 'counting based' or 'fast compact procedures' models. The goal of the present study was not to arbitrate between different cognitive models of mental arithmetic, and we used the *min* operand as a numerical index of problem-size/difficulty, merely because it was by far the best predictor of RT.

Next, we investigated if, how and when the *min* operand modulated the activity in the LPC and VTC arithmetic-selective regions. As predicted, we found several sites in aIPS and SPL in which the total HFB activity (integral of HFB power across the whole trial from stimuli onset to subject's RT) increased as a function of problem-size/difficulty, indexed as the magnitude of the min operand, while the initial activity remained constant. These results replicate previous fMRI findings (De Smedt et al., 2011; Dehaene et al., 1999; Kanjlia et al., 2016; Molko et al., 2003; Visscher et al., 2015), but with a much greater level of anatomical and temporal precision and at the single-subject level.

1
2
3 442 Importantly, once we regressed out the effect of RT, the modulation of total activity
4
5 443 in aIPS and SPL by *min* operand vanished, suggesting that that the aIPS and SPL are
6
7 444 engaged in the calculation process itself and are directly linked to behavioral RT
8
9 445 modulations. One possibility is that aIPS and SPL may be involved in the slow
10
11 446 accumulation of evidence needed to achieve a decision (Gonzalez et al., 2015; Tosoni,
12
13 447 Galati, Romani, & Corbetta, 2008), in this case about the truth of an arithmetic problem.
14
15 448 Future work could capitalize on the high signal-to-noise ratio and temporal and spatial
16
17 449 resolution of iEEG to test accumulation-of-evidence models (Dehaene, 2007; Gold &
18
19 450 Shadlen, 2007), using simpler numerical tasks such as number comparison or single-
20
21 451 digit arithmetic.

22
23
24 452 Note that in the present study, LPC contained sites whose total HFB activity in a
25
26 453 trial was positively correlated with *min* operand, yet which were not selective for
27
28 454 arithmetic processing (e.g., were active during both arithmetic and memory trials).
29
30 455 Those sites might therefore have been engaged in sustained attention, decision-making,
31
32 456 motor preparation, or some other non-arithmetic related process.

33
34
35 457 Recent iEEG findings revealed the existence of neuronal populations in the pITG
36
37 458 that selectively respond to Arabic numerals (NFA) as compared to other similar stimuli,
38
39 459 such as letters (Shum et al., 2013). However, subsequent iEEG studies showed that
40
41 460 responses to numerals in the VTC are more complex than what it was previously
42
43 461 predicted by the Triple-Code model (Dehaene & Cohen, 1995), by revealing that,
44
45 462 adjacent to the NFA, there are neuronal populations that respond to numerals more
46
47 463 strongly (Hermes et al., 2015) or even exclusively (Daitch et al., 2016) when they are in
48
49 464 the context of calculation, possibly reflecting top-down modulation coming from the LPC.
50
51
52
53
54
55
56
57
58
59
60

1
2
3
4
5
6
7
8
9
10
11
12
13
14
15
16
17
18
19
20
21
22
23
24
25
26
27
28
29
30
31
32
33
34
35
36
37
38
39
40
41
42
43
44
45
46
47
48
49
50
51
52
53
54
55
56
57
58
59
60

Furthermore, recent fMRI studies showed that voxels around the pITG are also active for number processing in blind subjects who learned to associated number shapes with sounds (Abboud, Maidenbaum, Dehaene, & Amedi, 2015) and when professional mathematicians evaluate high-level mathematical statements auditorily presented (Amalric & Dehaene, 2016). These results suggest that pITG might be involved in calculation beyond visual recognition of mathematical objects.

However, the precise role of pITG was not carefully examined, since none of the prior studies investigated if, how and when activity in pITG is modulated by numerical features of the calculations. Our results showed a surprising and unpredicted new effect in several pITG sites: a parametrical decrease in the initial activity (within one second of stimulus onset) as a function of problem-size/difficulty, while the total activity remained constant. This suggests that pITG engagement in multi-digit calculation are directly linked to quantity-related features of calculations and do not simply reflect top-down attentional modulation or sustained working memory subserving regions that execute the actual computation. If that was the case, the total activity in pITG, as in the aIPS and SPL, should have increased as a function of *min* operand. Crucially, since fMRI is only sensitive to the activity integrated over a temporal window of several seconds, the initial modulation observed in pITG would be undetectable with fMRI. This may explain why previous fMRI studies did not observe modulation in the pITG by arithmetic problem-size, but exclusively in a parietal-frontal network, including mainly the bilateral aIPS and SPL and the left inferior frontal gyrus (Kanjlia et al., 2016; Molko et al., 2003; Stanescu-Cosson et al., 2000).

The paradigm used in the present study, which involves judging the correctness of a

problem, is likely to involve several processing stages: recognizing the numbers involved in the problem, computing the sum of the two operands, and comparing the sum with the proposed result. Although our study cannot explicitly separate the neural processes corresponding to these stages, it seems likely that the *min*-related activity observed in pITG sites is primarily related to an early stage since, first, the most salient effects are observed during the beginning of a trial, and second, the *min* effect remained at most sites even after regressing out the effect of RT, while we would expect the calculation and decision-related processes to be correlated with RT.

Why would pITG activity related to calculation decrease for more difficult problems? Simple arithmetic problems appear to induce a temporal concentration of activity into a fast and strong initial peak. Conversely, for more complex problems, the same total amount of activity appeared to be diluted in time. These findings suggest that pITG may index the difficulty or amount of evidence available for a calculation problem. In this respect, our findings, in a high-level semantic task, parallel the observations made during perceptual decision-making tasks, for instance the fact that activity in area MT indexes the amount of perceptual evidence for a motion-based decision and therefore varies inversely with task difficulty (Britten, Shadlen, Newsome, & Movshon, 1993). A possible alternative interpretation could be that the higher initial activity observed in the pITG for smaller *min* operands reflects tuning to more familiar symbols, since it is known that the frequency of number words and digits decrease as a function of numerosity (Dehaene & Mehler, 1992). However, an important argument against this interpretation is the fact that the pITG sites that showed a decreased initial activity as a function of *min* operand falls adjacent to, but not directly in the 'number form area' and

do not show selective responses to isolated numerals as compared to other similar visual objects. Crucially, even the pITG sites that were active during Arabic digit recognition, did not show any modulation by the magnitude of the numbers, that is, they equally responded to digits ranging from 1-9. Furthermore, as all elements of the addition were presented simultaneously in the screen, is very unlikely that the pITG would be tuned to the frequency of only one of the elements, especially since the min operand appeared as the first operand in half of the trials and as second operand in the other half. Another possibility is that pITG stores visual representations the whole addition problem, as suggested by an early fMRI study (Rickard et al., 2000). In this case, the pITG modulation could potentially reflect the frequency of individual problem. Further studies, using a larger stimuli list and more adapted experimental design should try to arbitrate between these competing hypotheses.

Overall, we found a clear dissociation between the pattern of modulation by problem-size/difficulty in LPC and VTC. However, a couple of sites in the LPC also showed significant decreased initial activity as a function of min operand, similarly to the modulation observed in pITG. This might reflect the existence of functional connectivity between some neuronal populations in pITG and aIPS, as previously reported (Daitch et al., 2016). In the present study, however, only a single subject had simultaneous coverage of VTC and LPC and exhibited distinct sites with decreased pITG initial activity and increased IPS total activity as a function of *min* operand. Consequently, we could not systematically investigate how the functional profiles of LPC and VTC differ within subjects and, importantly, how these two distinct regions interact.

1
2
3 533 In sum, our results confirmed the selective engagement of aIPS and SPL in mental
4
5 534 calculation and reveal an unexpected pattern of parametric modulation in pITG, possibly
6
7 535 reflecting a role in the early identification of the difficulty/amount of evidence associated
8
9 536 with a given computation. In the absence of reported bilateral focal lesions in the pITG
10
11 537 region, its role in calculations remained unsuspected by previous neuropsychological
12
13 538 studies (Cappelletti, 2015, for a recent review) and asks for a re-evaluation of the
14
15 539 neurocognitive models of arithmetic and acquired and developmental dyscalculia.
16
17 540 Updated models should incorporate the pITG as an important hub for mental calculation
18
19 541 and any future studies on numerical cognition should include it as a ROI. More broadly,
20
21 542 our results challenge the classical view of ventral temporal cortex as the last stage of
22
23 543 the visual object categorization network, and shows that it contains regions crucially
24
25 544 involved in mathematical processing.
26
27
28
29
30
31 545
32
33 546
34
35 547
36
37
38
39
40
41
42
43
44
45
46
47
48
49
50
51
52
53
54
55
56
57
58
59
60

References

Amalric, M., & Dehaene, S. (2016). Origins of the brain networks for advanced mathematics in expert mathematicians. *Proceedings of the National Academy of Sciences of the United States of America*, 113(18), 4909–4917. <http://doi.org/10.1073/pnas.1603205113>

Arsalidou, M., & Taylor, M. J. (2011). Is 2+2=4? Meta-analyses of brain areas needed for numbers and calculations. *NeuroImage*, 54(3), 2382–2393. <http://doi.org/10.1016/j.neuroimage.2010.10.009>

Ashcraft, M. H. (1992). Cognitive arithmetic: a review of data and theory. *Cognition*, 44(1–2), 75–106.

Barrouillet, P., & Thevenot, C. (2013). On the problem-size effect in small additions: Can we really discard any counting-based account? *Cognition*, 128(1), 35–44. <http://doi.org/10.1016/j.cognition.2013.02.018>

Brainard, D. H. (1997). The Psychophysics Toolbox. *Spatial Vision*, 10(4), 433–436. <http://doi.org/10.1163/156856897X00357>

Britten, K. H., Shadlen, M. N., Newsome, W. T., & Movshon, J. A. (1993). Responses of neurons in macaque MT to stochastic motion signals. *Visual Neuroscience*, 10(6), 1157–1169.

Cappelletti, M. (2015). The Neuropsychology of Acquired Number and Calculation Disorders. In R. Cohen-Kadosh & A. Dowker (Eds.), *The Oxford Handbook of Numerical Cognition* (pp. 808–836). Oxford University Press.

Daitch, A. L., Foster, B. L., Schrouff, J., Rangarajan, V., Kasikci, I., Gattas, S., ... Parvizi, J. (2016). Mapping human temporal and parietal neuronal population activity and

- functional coupling during mathematical cognition. *Proceedings of the National Academy of Sciences*, 113(46), 201608434. <http://doi.org/10.1073/pnas.1608434113>
- De Smedt, B., Holloway, I. D., & Ansari, D. (2011). Effects of problem size and arithmetic operation on brain activation during calculation in children with varying levels of arithmetical fluency. *NeuroImage*, 57(3), 771–781. <http://doi.org/10.1016/j.neuroimage.2010.12.037>
- Dehaene, S. (2007). Symbols and Quantities in Parietal Cortex: Elements of a Mathematical Theory of Number Representation and Manipulation. In P. Haggard, Y. Rossetti, & M. Kawato (Eds.), *Attention & Performance XXII: Sensorimotor Foundations of Higher Cognition*. (pp. 527–574). Cambridge (UK): Oxford University Press.
- Dehaene, S., & Cohen, L. (1995). Towards an anatomical and functional model of number processing. *Mathematical Cognition*.
- Dehaene, S., & Mehler, J. (1992). Cross-linguistic regularities in the frequency of number words. *Cognition*, 43(1), 1–29.
- Dehaene, S., Piazza, M., Pinel, P., & Cohen, L. (2003). Three Parietal Circuits for Number Processing. *Cognitive Neuropsychology*, 20(3–6), 487–506. <http://doi.org/10.1080/02643290244000239>
- Dehaene, S., Spelke, E., Pinel, P., Stanescu, R., & Tsivkin, S. (1999). Sources of mathematical thinking: behavioral and brain-imaging evidence. *Science (New York, N.Y.)*, 284(5416), 970–974. <http://doi.org/10.1126/science.284.5416.970>
- Della Puppa, A., De Pellegrin, S., d'Avella, E., Giofrè, G., Munari, M., Saladini, M., ...

- 594 Semenza, C. (2013). Right parietal cortex and calculation processing:
595 intraoperative functional mapping of multiplication and addition in patients affected
596 by a brain tumor. *Journal of Neurosurgery*, 119(5), 1107–1111.
597 <http://doi.org/10.3171/2013.6.JNS122445>
- 598 Foster, B. L., Rangarajan, V., Shirer, W. R., & Parvizi, J. (2015). Intrinsic and task-
599 dependent coupling of neuronal population activity in human parietal cortex.
600 *Neuron*, 86(2), 578–590. <http://doi.org/10.1016/j.neuron.2015.03.018>
- 601 Gold, J. I., & Shadlen, M. N. (2007). The neural basis of decision making. *Annual*
602 *Review of Neuroscience*, 30, 535–574.
603 <http://doi.org/10.1146/annurev.neuro.29.051605.113038>
- 604 Gonzalez, A., Hutchinson, J. B., Uncapher, M. R., Chen, J., LaRocque, K. F., Foster, B.
605 L., ... Wagner, A. D. (2015). Electrocorticography reveals the temporal dynamics of
606 posterior parietal cortical activity during recognition memory decisions. *Proceedings*
607 *of the National Academy of Sciences of the United States of America*, 112(35),
608 11066–11071. <http://doi.org/10.1073/pnas.1510749112>
- 609 Grill-Spector, K., & Weiner, K. S. (2014). The functional architecture of the ventral
610 temporal cortex and its role in categorization. *Nature Reviews. Neuroscience*, 15(8),
611 536–548. <http://doi.org/10.1038/nrn3747>
- 612 Groen, G. J., & Parkman, J. M. (1972). A chronometric analysis of simple addition.
613 *Psychological Review*, 79(4), 329–343. <http://doi.org/10.1037/h0032950>
- 614 Grotheer, M., Jeska, B., & Grill-Spector, K. (2018). A preference for mathematical
615 processing outweighs the selectivity for Arabic numbers in the inferior temporal
616 gyrus. *NeuroImage*, 175, 188–200.

- 617 <http://doi.org/10.1016/j.neuroimage.2018.03.064>
- 618 Hannagan, T., Amedi, A., Cohen, L., Dehaene-Lambertz, G., & Dehaene, S. (2015).
619 Origins of the specialization for letters and numbers in ventral occipitotemporal
620 cortex. *Trends in Cognitive Sciences*. <http://doi.org/10.1016/j.tics.2015.05.006>
- 621 Harvey, B. M., Ferri, S., & Orban, G. A. (2017). Comparing Parietal Quantity-
622 Processing Mechanisms between Humans and Macaques Two Quantity-
623 Processing Networks in Human Parietal Cortex: a Proposal, *21*(10), 779–793.
624 <http://doi.org/10.1016/j.tics.2017.07.002>
- 625 Harvey, B. M., Klein, B. P., Petridou, N., & Dumoulin, S. O. (2013). Topographic
626 Representation of Numerosity in the Human Parietal Cortex. *Science*, *341*(6150),
627 1123–1126. <http://doi.org/10.1126/science.1239052>
- 628 Hermes, D., Miller, K. J., Noordmans, H. J., Vansteensel, M. J., & Ramsey, N. F. (2010).
629 Automated electrocorticographic electrode localization on individually rendered
630 brain surfaces. *Journal of Neuroscience Methods*, *185*(2), 293–298.
631 <http://doi.org/10.1016/j.jneumeth.2009.10.005>
- 632 Hermes, D., Rangarajan, V., Foster, B. L., King, J.-R., Kasikci, I., Miller, K. J., & Parvizi,
633 J. (2015). Electrophysiological Responses in the Ventral Temporal Cortex During
634 Reading of Numerals and Calculation. *Cerebral Cortex (New York, N.Y. : 1991)*.
635 <http://doi.org/10.1093/cercor/bhv250>
- 636 Kanjlia, S., Lane, C., Feigenson, L., & Bedny, M. (2016). Absence of visual experience
637 modifies the neural basis of numerical thinking. *Proceedings of the National*
638 *Academy of Sciences*, *113*(40), 201524982.
639 <http://doi.org/10.1073/pnas.1524982113>

- Knops, A., Thirion, B., Hubbard, E. M., Michel, V., & Dehaene, S. (2009). Recruitment of an area involved in eye movements during mental arithmetic. *Science (New York, N.Y.)*, 324(5934), 1583–5. <http://doi.org/10.1126/science.1171599>
- Logothetis, N. K., Pauls, J., Augath, M., Trinath, T., & Oeltermann, A. (2001). Neurophysiological investigation of the basis of the fMRI signal. *Nature*, 412(6843), 150–157. <http://doi.org/10.1038/35084005>
- Manning, J. R., Jacobs, J., Fried, I., & Kahana, M. J. (2009). Broadband shifts in local field potential power spectra are correlated with single-neuron spiking in humans. *The Journal of Neuroscience : The Official Journal of the Society for Neuroscience*, 29(43), 13613–13620. <http://doi.org/10.1523/JNEUROSCI.2041-09.2009>
- Menon, V., Rivera, S. M., White, C. D., Glover, G. H., & Reiss, A. L. (2000). Dissociating Prefrontal and Parietal Cortex Activation during Arithmetic Processing. *NeuroImage*, 12(4), 357–365. <http://doi.org/10.1006/nimg.2000.0613>
- Molko, N., Cachia, A., Bruandet, M., Bihan, D. Le, Cohen, L., & Dehaene, S. (2003). Functional and Structural Alterations of the Intraparietal Sulcus in a Developmental Dyscalculia of Genetic Origin. *Neuron*, 40, 847–858.
- Pallier, C., Devauchelle, A., & Dehaene, S. (2010). Cortical representation of the constituent structure of sentences. *PNAS*. <http://doi.org/10.1073/pnas.1018711108/-/DCSupplemental.www.pnas.org/cgi/doi/10.1073/pnas.1018711108>
- Parvizi, J., Jacques, C., Foster, B. L., Witthoft, N., Rangarajan, V., Weiner, K. S., & Grill-Spector, K. (2012). Electrical stimulation of human fusiform face-selective regions distorts face perception. *The Journal of Neuroscience : The Official Journal of the*

- 663 *Society for Neuroscience*, 32(43), 14915–14920.
664 <http://doi.org/10.1523/JNEUROSCI.2609-12.2012>
- 665 Piazza, M., Izard, V., Pinel, P., Le Bihan, D., & Dehaene, S. (2004). Tuning curves for
666 approximate numerosity in the human intraparietal sulcus. *Neuron*, 44(3), 547–555.
667 <http://doi.org/10.1016/j.neuron.2004.10.014>
- 668 Piazza, M., Pinel, P., Le Bihan, D., & Dehaene, S. (2007). A Magnitude Code Common
669 to Numerosities and Number Symbols in Human Intraparietal Cortex. *Neuron*, 53(2),
670 293–305. <http://doi.org/10.1016/j.neuron.2006.11.022>
- 671 Pinel, P., Dehaene, S., Rivie, D., & Lebihan, D. (2001). Modulation of Parietal Activation
672 by Semantic Distance in a Number Comparison Task. *Stimulus*, 1026, 1013–1026.
673 <http://doi.org/10.1006/nimg.2001.0913>
- 674 Pinheiro-Chagas, P., Dotan, D., Piazza, M., & Dehaene, S. (2017). Finger tracking
675 reveals the covert processing stages of mental arithmetic. *Open Mind: Discoveries*
676 *in Cognitive Science*, 1–12. http://doi.org/10.1162/OPMI_a_00003
- 677 Ray, S., & Maunsell, J. H. R. (2011). Different origins of gamma rhythm and high-
678 gamma activity in macaque visual cortex. *PLoS Biology*, 9(4), e1000610.
679 <http://doi.org/10.1371/journal.pbio.1000610>
- 680 Rickard, T. ., Romero, S. ., Basso, G., Wharton, C., Flitman, S., & Grafman, J. (2000).
681 The calculating brain: an fMRI study. *Neuropsychologia*, 38(3), 325–335.
682 [http://doi.org/10.1016/S0028-3932\(99\)00068-8](http://doi.org/10.1016/S0028-3932(99)00068-8)
- 683 Semenza, C., Salillas, E., De Pallegirin, S., & Della Puppa, A. (2017). Balancing the 2
684 Hemispheres in Simple Calculation: Evidence from Direct Cortical
685 Electrostimulation. *Cerebral Cortex*, 27(10), 4806–4814.

686 <http://doi.org/10.1093/cercor/bhw277>

687 Shum, J., Hermes, D., Foster, B. L., Dastjerdi, M., Rangarajan, V., Winawer, J., ...

688 Parvizi, J. (2013). A brain area for visual numerals. *The Journal of Neuroscience :*

689 *The Official Journal of the Society for Neuroscience*, 33(16), 6709–6715.

690 <http://doi.org/10.1523/JNEUROSCI.4558-12.2013>

691 Stanescu-Cosson, R., Pinel, P., van De Moortele, P. F., Le Bihan, D., Cohen, L., &

692 Dehaene, S. (2000). Understanding dissociations in dyscalculia: a brain imaging

693 study of the impact of number size on the cerebral networks for exact and

694 approximate calculation. *Brain: A Journal of Neurology*, 123 (Pt 1, 2240–55.

695 Retrieved from <http://www.ncbi.nlm.nih.gov/pubmed/11050024>

696 Tosoni, A., Galati, G., Romani, G. L., & Corbetta, M. (2008). Sensory-motor

697 mechanisms in human parietal cortex underlie arbitrary visual decisions. *Nature*

698 *Neuroscience*, 11(12), 1446–1453. <http://doi.org/10.1038/nn.2221>

699 Uittenhove, K., Thevenot, C., & Barrouillet, P. (2016). Fast automated counting

700 procedures in addition problem solving: When are they used and why are they

701 mistaken for retrieval? *Cognition*, 146, 289–303.

702 <http://doi.org/10.1016/j.cognition.2015.10.008>

703 Visscher, A. De, Berens, S. C., Keidel, J. L., Noël, M., Bird, C. M., De Visscher, A., ...

704 Bird, C. M. (2015). The interference effect in arithmetic fact solving: An fMRI study.

705 *NeuroImage*, 116, 92–101. <http://doi.org/10.1016/j.neuroimage.2015.04.063>

706 Zbrodoff, J. N., & Logan, G. D. (2005). What everyone finds: the problem size effect. In

707 J. I. D. Campbell (Ed.), *The Handbook of Mathematical Cognition* (pp. 331–345).

708 New York: Psychology Press.

709

710

For Review Only

1
2
3
4
5
6
7
8
9
10
11
12
13
14
15
16
17
18
19
20
21
22
23
24
25
26
27
28
29
30
31
32
33
34
35
36
37
38
39
40
41
42
43
44
45
46
47
48
49
50
51
52
53
54
55
56
57
58
59
60

711 **Figures**

712

For Review Only

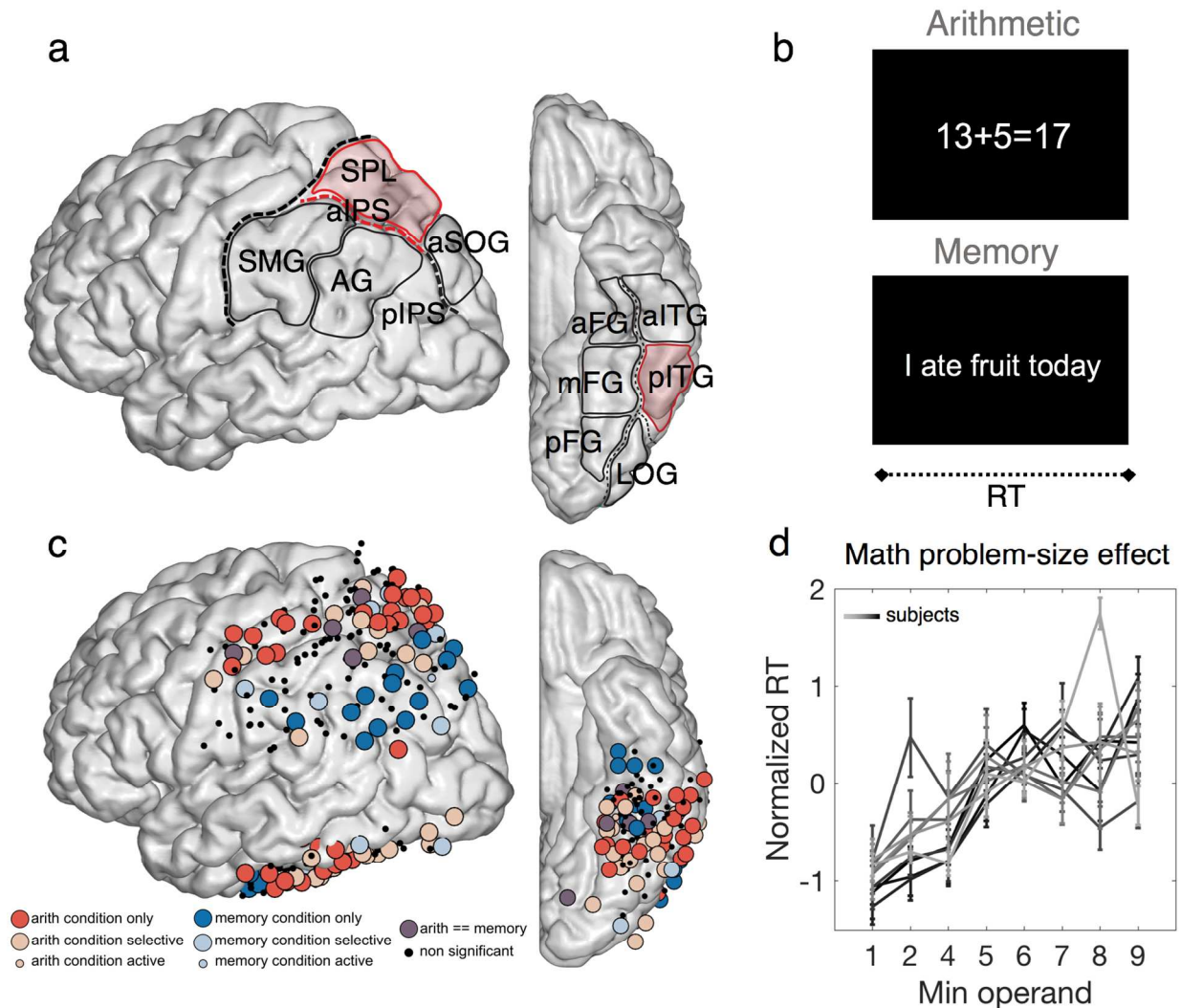


Figure 1. Anatomical subdivisions, task, recording sites, and behavioral problem-size effect. A) The anatomical subdivisions within the lateral parietal cortex (LPC) and ventral temporal cortex (VTC) considered in this study, as seen in the left hemisphere from a slightly posterior viewpoint. LPC: AG, angular gyrus; aIPS, anterior intraparietal sulcus; aSOG, anterior superior occipital gyrus; pIPS posterior intraparietal sulcus; SMG, supramarginal gyrus; SPL, superior parietal lobule. VTC: aFG, anterior fusiform gyrus; aITG, anterior inferior temporal gyrus; pFG, posterior fusiform gyrus; mFG, mid fusiform gyrus; pITG, posterior inferior temporal gyrus. Arithmetic-ROIs marked in red. B) Exemplar stimuli of the Memory & Arithmetic verification task. In each trial, subjects were asked to verify the correctness of visually presented additions or a memory statements, by pressing one of two buttons. C) LPC and VTC sites from all 10 subjects are projected onto a single left hemisphere using the MNI space (see *Electrodes Localization* in the Methods), with the color of each site indicating its selectivity for arithmetic versus memory. Bright blue and bright red mark the most selective sites, passing three criteria for significance (e.g. arithmetic > baseline; arithmetic > memory; and memory indistinguishable from baseline). Faded red and blue indicate the selective sites that met only the first two criteria. Small faded red and blue

1
2
3
4
5
6
7
8
9
10
11
12
13
14
15
16
17
18
19
20
21
22
23
24
25
26
27
28
29
30
31
32
33
34
35
36
37
38
39
40
41
42
43
44
45
46
47
48
49
50
51
52
53
54
55
56
57
58
59
60

731 indicate sites that met only the first criteria. Sites colored in purple were activated
732 similarly during the two conditions, and sites marked by small black dots were not
733 significantly active during either condition. Significance was defined as $P < 0.05$, FDR
734 corrected within subject. D) Behavioral problem-size effect (*min* operand) in each
735 subject (different shades of gray): average RT plotted as a function of *min* operand
736 (normalized within each subject by subtracting the mean and dividing by the standard
737 deviation).
738

For Review Only

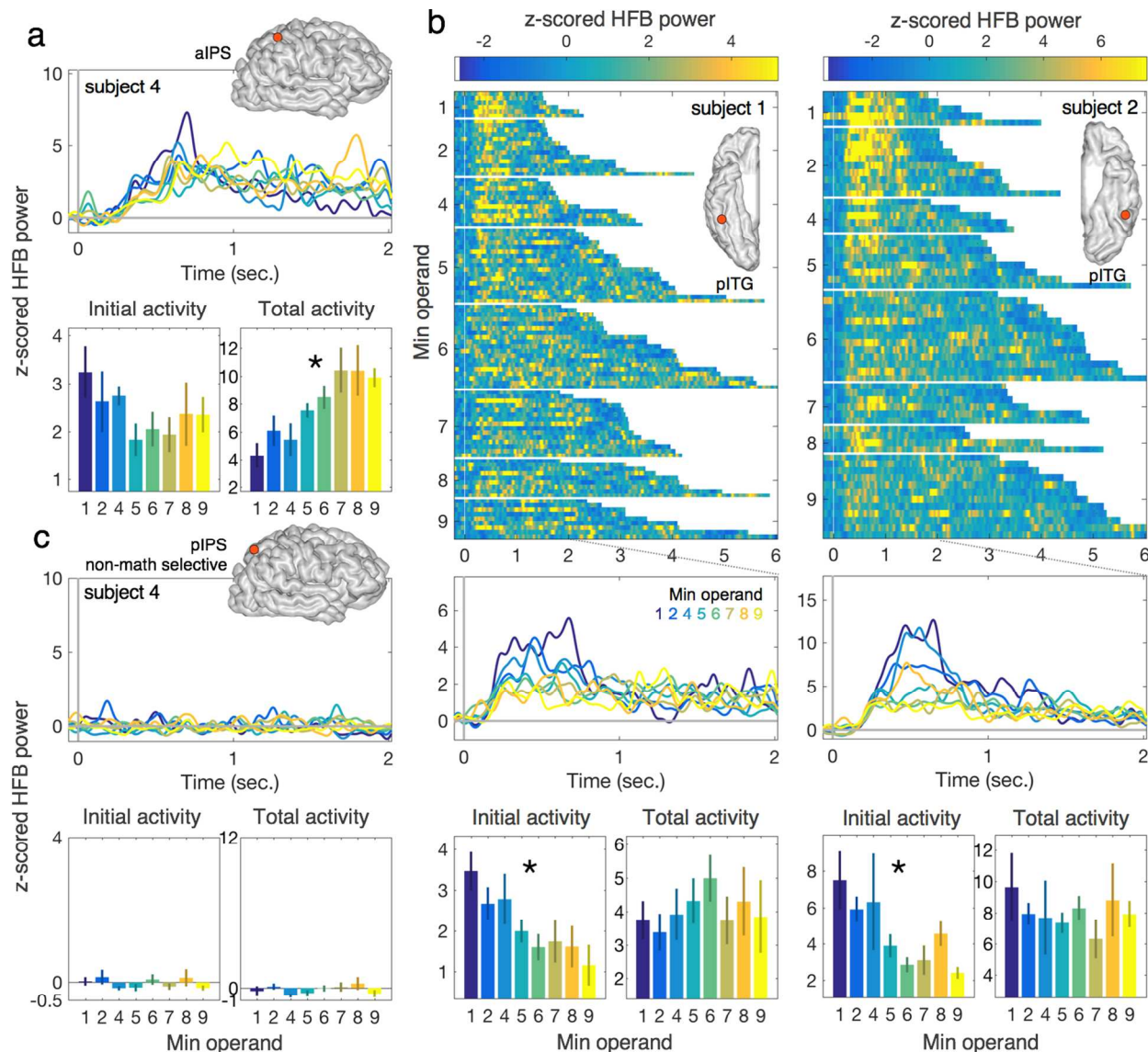


Figure 2. Example sites whose activity is modulated by the *min* operand. A) Exemplar arithmetic selective channel in the aIPS showing increased HFB total activity as a function of *min* operand. The time course shows the activity averaged across trials with a given *min* operand (zoomed in the first two seconds of the trial). Bar plots show average initial activity (within the first second of a trial), and average total activity (integrated over the whole trial) as a function of *min* operand. B) Two exemplar channels showing decreased HFB initial activity in the pITG as a function of *min* operand (both arithmetic selective, one in each hemisphere in two different subjects). The first plot in each column shows the time course of activity for each trial, sorted by *min* operand and then by RT. C) Exemplar channel of a non- arithmetic selective channel in the posterior IPS of the same subject as in B showing no HFB modulation by *min* operand. An asterisk indicates that a regression analysis found a significant effect of *min* operand on either initial or total HFB activity ($P < 0.05$, FDR corrected).

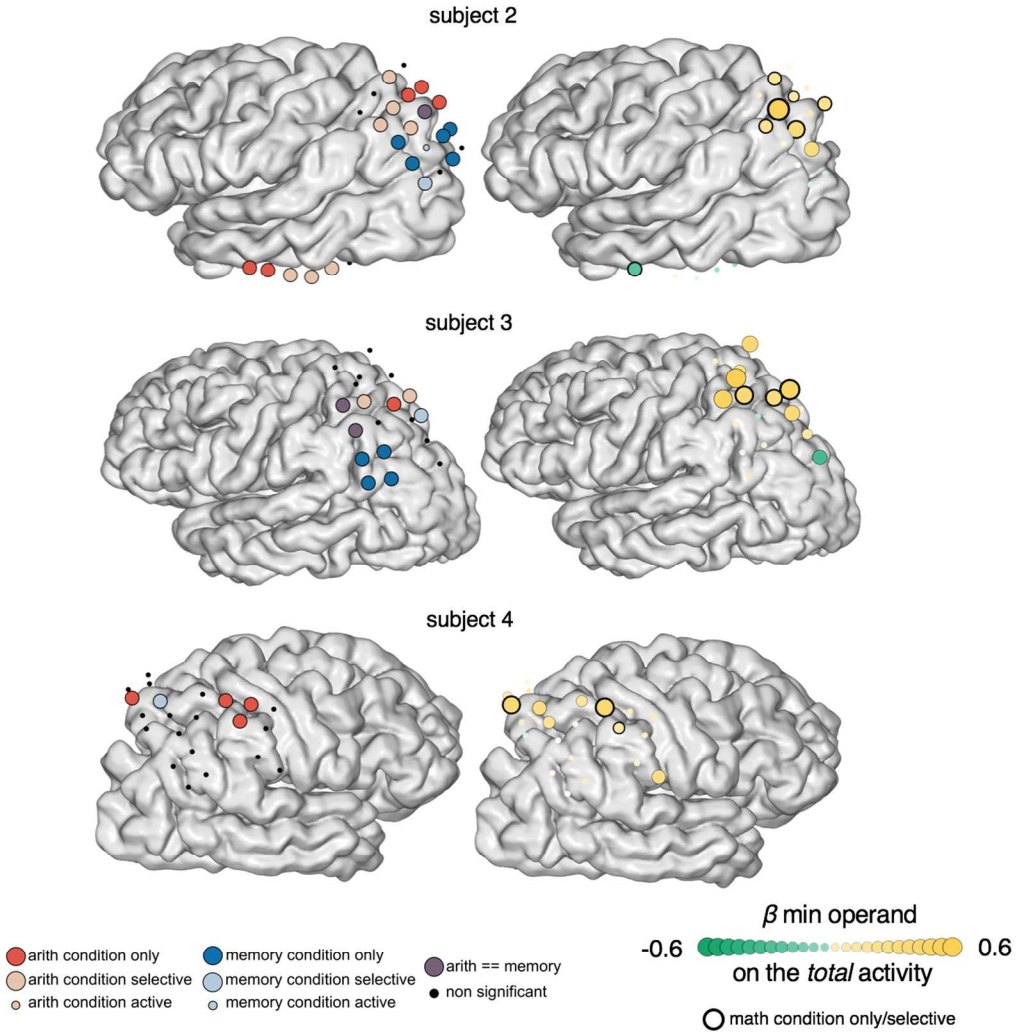


Figure 3. Anatomical and functional specificity of the HFB activity modulation in the LPC. The figure illustrates the relationship, in LPC, between (1) selectivity for arithmetic vs. memory (left brain, same color code as Figure 1B) and (2) the effect of the min operand on total activity (right brain). The figure shows all 3 (out of 7) subjects with LPC coverage who showed the effect. Most channels whose total activity increased with problem size were located within the aIPS and SPL and were arithmetic selective, but some channels that showed this effect felt outside aIPS and SPL and/or were not arithmetic selective. For the min effect, dot color indicates the size and sign of the regression coefficient and dot size indicates the size of the regression coefficient. A thick black ring indicate that the channel is also arithmetic selective. Small dots indicate non-significant channels. P-values were FDR-corrected within subject.

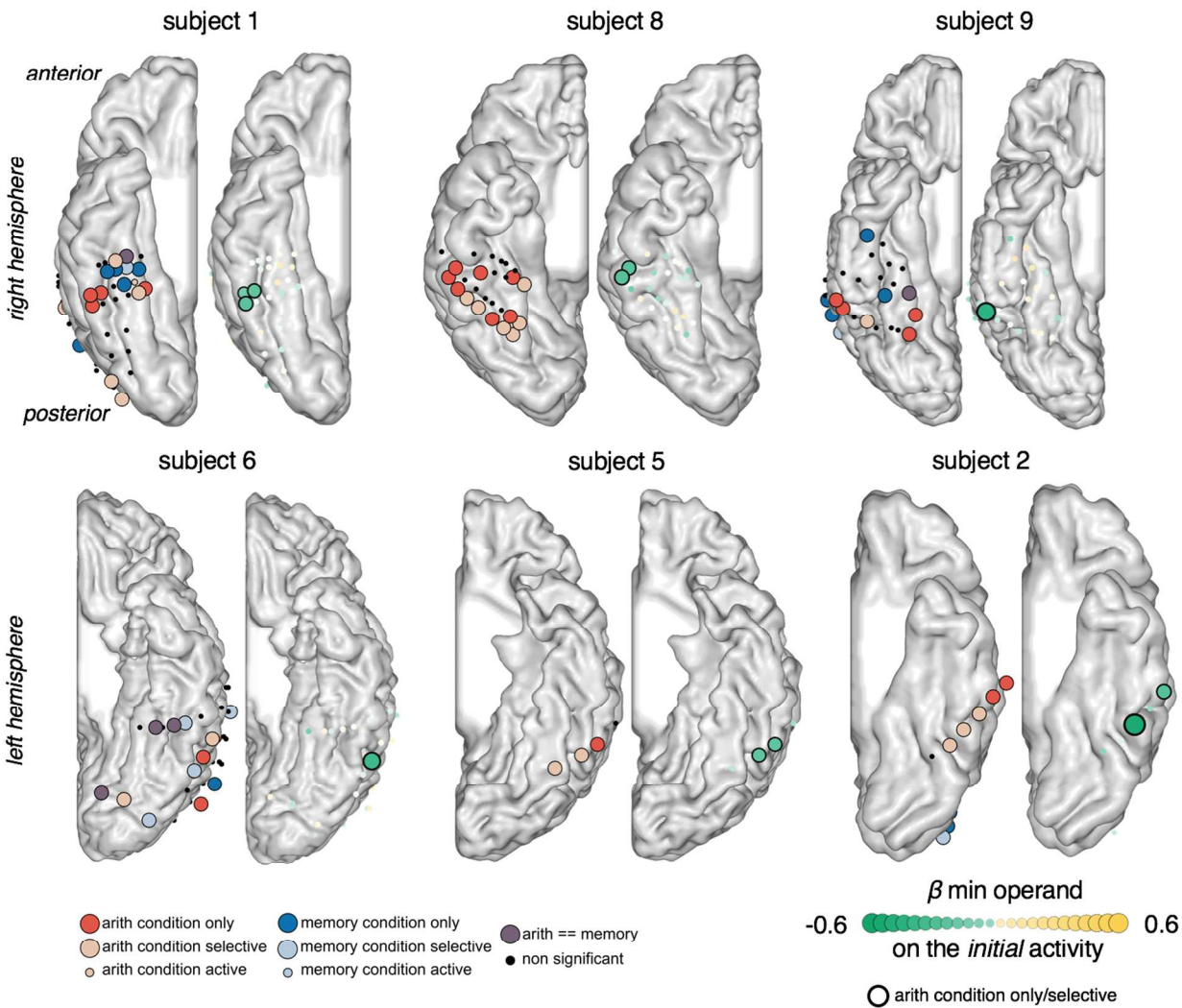


Figure 4. Anatomical and functional specificity of the HFB activity modulation in the VTC. The figure illustrates the relationship, in VTC, between (1) selectivity for arithmetic vs. memory (left brain, same color code as Figure 1b) and (2) the effect of the *min* operand on initial activity (right brain). The figure shows all 6 (out of 7) subjects with pITG coverage who showed the effect. All channels whose initial activity decreased with problem size were located within the pITG (except for the most anterior channel of subject 2 - anterior ITG - and were arithmetic selective (thick black ring). For the *min* effect, dot color indicates the size and sign of the regression coefficient and dot size indicates the size of the regression coefficient (standardized) ($P < 0.05$, FDR corrected). Small dots indicate non-significant channels.

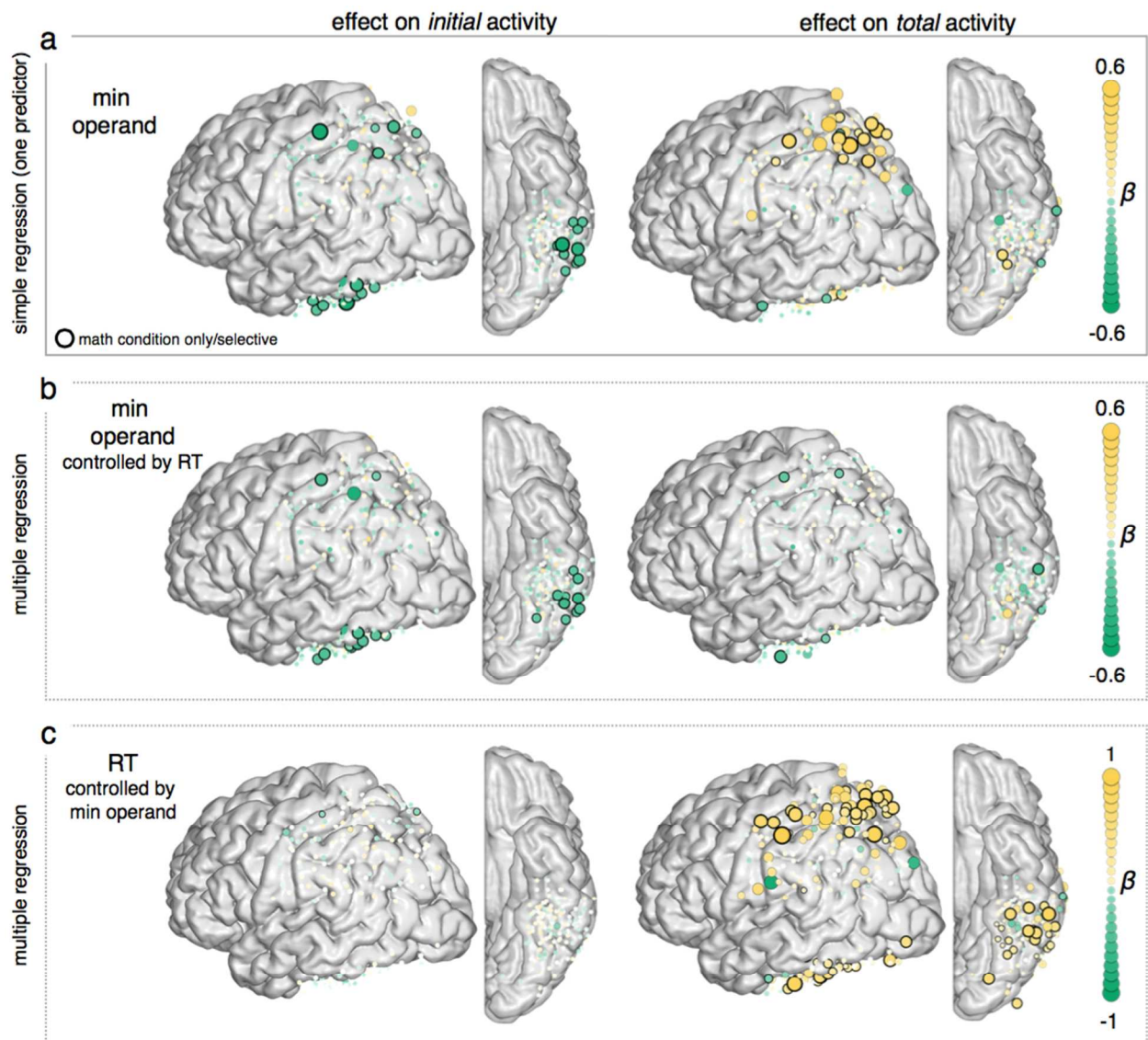


Figure 5. Modulation by *min* operand and RT in the LPC and VTC. Regression analysis, where activity is modeled as a function of *min operand* in the initial activity (within the first second of a trial, left column) and total activity (integrated over the whole trial, right column). A) The effect of the *min* operand in a simple regression (one predictor). B) The effect of the *min* operand in a multiple regression that included both the *min* operand and the RT as predictors. C) The effect of the RT in a multiple regression that included both the *min* operand and the RT as predictors. For all plots, dot color indicates the size and sign of the regression coefficient and dot size indicates the size of the regression coefficient significant (standardized). A thick black ring indicate that the channel is also arithmetic selective. Small dots indicate non-significant channels. Significance: $P < 0.05$, FDR corrected.

Tables

792
793

For Review Only

1
2
3
4
5
6
7
8
9
10
11
12
13
14
15
16
17
18
19
20
21
22
23
24
25
26
27
28
29
30
31
32
33
34
35
36
37
38
39
40
41
42
43
44
45
46
47
48
49
50
51
52
53
54
55
56
57
58
59
60

794 **Table 1. Stimuli list for the Arithmetic task.**

10+1=11	78+2=80	4+25=29	5+87=92	56+6=62	24+7=31	16+8=24	45+9=54
1+18=19	78+2=65	4+25=32	5+87=93	56+6=64	26+7=33	16+8=22	45+9=55
1+18=25	2+52=54	24+5=29	28+6=34	67+6=73	26+7=34	47+8=55	47+9=56
1+41=42	2+52=56	24+5=39	28+6=36	6+22=28	59+7=66	47+8=54	47+9=56
1+41=50	2+60=62	33+5=38	38+6=44	6+22=33	59+7=65	8+30=38	53+9=62
11+2=16	2+60=72	33+5=32	38+6=42	6+36=42	7+34=41	8+30=45	53+9=63
24+2=26	20+4=24	81+5=86	42+6=48	6+36=43	7+34=42	8+65=73	9+23=32
24+2=19	20+4=17	81+5=92	42+6=59	6+39=45	7+43=50	8+65=74	9+23=34
61+2=63	54+4=58	5+63=68	51+6=57	6+39=47	7+43=63	44+9=53	9+86=95
61+2=75	54+4=65	5+63=56	51+6=71	24+7=31	7+67=73	44+9=51	9+86=96

795
796

For Review Only

Table 2. Subject demographics and behavioral performance.

Subject	Gender	Age	IQ	Handedness	Hemi	Behavior Performance		
						Arith Acc (%)	Avg Arith RT (s)	Avg Memory RT (s)
S1	M	41	129	R	R	96	3.18	2.15
S2	F	36	N/A	R	L	95	3.69	2.1
S3	F	22	N/A	R	L	89	5.78	3.12
S4	M	46	N/A	A	R	93	5.24	3.38
S5	F	31	71	R	L	63	3.61	3.11
S6	M	29	77	R	L	88	2.85	3.13
S7	M	47	74	L	L	96	3.3	3.23
S8	M	67	N/A	R	R	94	2.02	2.84
S9	F	65	113	R	R	80	3.28	2.35

This table shows the gender, age at time of surgery, IQ (N/A indicates that the IQ test was not performed before surgery), handedness (R, right-handed; L, left-handed; A, ambidextrous) and Hemi (hemisphere of coverage) of all subjects participating in study. It also shows the accuracy and average reaction time (RT) for each condition (Arithmetic and Memory).

1
2
3
4
5
6
7
8
9
10
11
12
13
14
15
16
17
18
19
20
21
22
23
24
25
26
27
28
29
30
31
32
33
34
35
36
37
38
39
40
41
42
43
44
45
46
47
48
49
50
51
52
53
54
55
56
57
58
59
60

803 **Table 3. Arithmetic problem-size effect by subject.**

Subject	Min operand				Max operand				Sum				Absolute deviant			
	Beta	In	t	p	Beta	In	t	p	Beta	In	t	p	Beta	In	t	p
S1	0.45	✓	5.55	1.7E-07	0.08	-	0.99	0.32	-0.02	-	-0.29	0.78	0.08	-	0.99	0.32
S2	0.58	✓	6.30	1.6E-08	0.08	-	0.82	0.41	0.05	-	0.52	0.60	0.08	-	0.82	0.41
S3	0.71	✓	8.76	3.5E-13	0.13	-	1.68	0.10	0.03	-	0.34	0.74	0.14	-	1.68	0.10
S4	0.40	✓	4.11	1.0E-04	0.00	-	0.00	1.00	0.16	-	1.61	0.11	0.31	✓	3.15	2.4E-03
S5	0.05	-	0.41	0.68	-0.01	-	-0.07	0.94	0.29	✓	2.63	1.0E-02	0.00	-	-0.02	0.98
S6	0.32	✓	3.01	3.5E-03	0.07	-	0.69	0.49	0.02	-	0.16	0.87	0.08	-	0.69	0.49
S7	0.47	✓	4.43	3.1E-05	0.12	-	1.16	0.25	0.15	-	1.36	0.18	0.12	-	1.16	0.25
S8	0.37	✓	3.58	6.1E-04	0.00	-	0.00	1.00	0.31	✓	3.05	3.2E-03	0.29	✓	2.92	4.7E-03
S9	0.44	✓	4.01	1.4E-04	-0.10	-	-0.96	0.34	0.04	-	0.31	0.88	-0.01	-	-0.96	0.34
S10	0.53	✓	5.38	8.1E-07	0.00	-	0.00	1.00	-0.15	-	-1.44	0.15	0.15	-	1.67	0.09

804 This table shows the statistics of the stepwise regression analysis, which included the RT as the
805 dependent variable and the min operand, max operand, sum and absolute deviant as predictors. 'In'
806 indicates if the predictor was included (✓, $p < 0.05$) or not (-) in the final model.
807
808

Table 4. Number of electrodes showing *arithmetic* selectivity and modulation by the min operand, by subject/anatomical region.

Subject	Hemi	pITG						aIPS						aSPL					
		TOT	AA	AS	AO	DecIN	IncTO	TOT	AA	AS	AO	DecIN	IncTO	TOT	AA	AS	AO	DecIN	IncTO
S1	R	5	3	3	3	3,3,3	-,-,-	6	2	2	2	-,-,-	-,-,-	8	3	2	1	-,-,-	-,-,-
S2	L	2	2	2	-	1,1,-	-,-,-	4	2	2	-	1,1,-	2,2,-	8	6	5	3	1,1,1	4,4,2
S3	L	-	-	-	-	-,-,-	-,-,-	3	2	1	-	-,-,-	2,1,-	7	2	2	1	-,-,-	2,2,1
S4	R	-	-	-	-	-,-,-	-,-,-	4	2	2	2	-,-,-	1,1,1	7	1	1	1	-,-,-	1,1,1
S5	L	3	2	2	1	2,2,1	-,-,-	-	-	-	-	-,-,-	-,-,-	5	2	2	2	1,1,1	-,-,-
S6	L	5	4	2	1	1,1,1	-,-,-	5	3	3	2	1,1,1	-,-,-	12	5	5	5	-,-,-	-,-,-
S7	L	4	1	1	1	-,-,-	-,-,-	4	-	-	-	-,-,-	-,-,-	5	-	-	-	-,-,-	-,-,-
S8	R	6	5	5	3	2,2,2	-,-,-	-	-	-	-	-,-,-	-,-,-	-	-	-	-	-,-,-	-,-,-
S9	R	3	2	2	2	1,1,1	-,-,-	4	2	1	-	-,-,-	-,-,-	1	-	-	-	-,-,-	-,-,-
S10	L	-	-	-	-	-,-,-	-,-,-	3	1	1	1	-,-,-	-,-,-	-	-	-	-	-,-,-	-,-,-
TOTAL		28	19	17	11	10,10,8	-,-,-	33	14	12	7	2,2,1	5,4,1	53	19	17	13	2,2,2	7,7,4

Hemi, hemisphere; TOT, total number of electrodes; AA, arithmetic condition active (relative to baseline); AS, arithmetic condition selective (relative to baseline and memory); AO, arithmetic condition only (arithmetic selective and memory not active relative to baseline); DecIN, decreased initial activity as a function of min operand; IncTO, increased total activity as a function of min operand. The numbers separated by commas correspond to AA, AS, AO respectively. Electrodes included are statistically significant at $p < 0.05$ FDR-corrected within subject.

1
2
3 819
4
5 820
6
7 821

Table 5. Number of electrodes showing *memory* selectivity and modulation by the min operand, by subject/anatomical region.

Subject	Hemi	pITG						aIPS						SPL					
		TOT	MA	MS	MO	DecIN	IncTO	TOT	MA	MS	MO	DecIN	IncTO	TOT	MA	MS	MO	DecIN	IncTO
S1	R	5	-	-	-	-,-,-	-,-,-	6	-	-	-	-,-,-	-,-,-	8	3	1	-	-,-,-	-,-,-
S2	L	2	2	-	-	1,-,-	-,-,-	4	3	1	1	1,-,-	2,-,-	8	3	-	-	-,-,-	2,-,-
S3	L	-	-	-	-	-,-,-	-,-,-	3	1	-	-	-,-,-	1,-,-	7	1	-	-	-,-,-	1,-,-
S4	R	-	-	-	-	-,-,-	-,-,-	4	-	-	-	-,-,-	-,-,-	7	1	1	-	-,-,-	1,1,-
S5	L	3	1	-	-	1,-,-	-,-,-	-	-	-	-	-,-,-	-,-,-	5	-	-	-	-,-,-	-,-,-
S6	L	5	2	2	-	-,-,-	-,-,-	5	-	-	-	-,-,-	-,-,-	12	-	-	-	-,-,-	-,-,-
S7	L	4	-	-	-	-,-,-	-,-,-	4	-	-	-	-,-,-	-,-,-	5	-	-	-	-,-,-	-,-,-
S8	R	6	2	-	-	-,-,-	-,-,-	-	-	-	-	-,-,-	-,-,-	-	-	-	-	-,-,-	-,-,-
S9	R	3	-	-	-	-,-,-	-,-,-	4	1	-	-	-,-,-	-,-,-	1	-	-	-	-,-,-	-,-,-
S10	L	-	-	-	-	-,-,-	-,-,-	3	-	-	-	-,-,-	-,-,-	-	-	-	-	-,-,-	-,-,-
TOTAL		28	7	2	-	2,-,-	-,-,-	33	5	1	1	1,-,-	3,-,-	53	8	2	-	-,-,-	4,1,-

822
823 Hemi, hemisphere; TOT, total number of electrodes; MA, memory condition active (relative to baseline);
824 MS, memory condition selective (relative to baseline and arithmetic); MO, memory condition only
825 (memory selective and arithmetic not active relative to baseline); DecIN, decreased initial activity as a
826 function of min operand; IncTO, increased total activity as a function of min operand. The numbers
827 separated by commas correspond to MA, MS, MO respectively. Electrodes included are statistically
828 significant at $p < 0.05$ FDR-corrected within subject
829

Table 6. Number of electrodes showing modulation by the *min* operand by subject in other anatomical regions

Subject	Hemi	Other anatomical regions (outside pITG, aIPS and SPL)										
		TOT	AA	AS	AO	DecIN	IncTO	MA	MS	MO	DecIN	IncTO
S1	R	45	10	7	2	1,1,1	-,-,-	10	7	6	-,-,-	-,-,-
S2	L	12	3	3	2	1,1,1	-,-,-	7	5	4	-,-,-	1,-,-
S3	L	9	1	-	-	-,-,-	-,-,-	6	5	4	-,-,-	-,-,-
S4	R	11	1	1	1	-,-,-	1,1,1	-	-	-	-,-,-	-,-,-
S5	L	1	1	1	-	-,-,-	-,-,-	1	-	-	-,-,-	-,-,-
S6	L	26	8	3	1	-,-,-	-,-,-	7	3	1	-,-,-	-,-,-
S7	L	9	2	2	1	-,-,-	-,-,-	-	-	-	-,-,-	-,-,-
S8	R	20	8	8	4	-,-,-	2,2,1	4	-	-	-,-,-	1,-,-
S9	R	23	4	3	2	-,-,-	-,-,-	6	5	4	-,-,-	-,-,-
S10	L	12	1	1	-	-,-,-	-,-,-	4	3	3	-,-,-	-,-,-
TOTAL		168	39	29	13	2,2,2	3,3,2	45	28	22	-,-,-	2,-,-

Hemi, hemisphere; TOT, total number of electrodes; AA, arithmetic condition active (relative to baseline); MS, arithmetic condition selective (relative to baseline and memory); AO, arithmetic condition only (arithmetic selective and memory not active relative to baseline); MA, memory condition active (relative to baseline); MS, memory condition selective (relative to baseline and arithmetic); MO, memory condition only (memory selective and arithmetic not active relative to baseline); DecIN, decreased initial activity as a function of min operand; IncTO, increased total activity as a function of min operand. The numbers separated by commas correspond to AA, AS, AO or MA, MS, MO respectively. Electrodes included are statistically significant at $p < 0.05$ FDR-corrected within subject.

1
2
3
4
5
6
7
8
9
10
11
12
13
14
15
16
17
18
19
20
21
22
23
24
25
26
27
28
29
30
31
32
33
34
35
36
37
38
39
40
41
42
43
44
45
46
47
48
49
50
51
52
53
54
55
56
57
58
59
60

Table 7. Selectivity and modulation related to the recognition of Arabic numerals in the VTC channels that showed decreased initial activity as a function of *min* operand.

Subject	Hemi	Region	Numeral active	Numeral selective	Modulation by numeral
S1	R	pITG	✓	-	-
S1	R	pITG	✓	-	-
S1	R	pITG	-	-	-
S2	L	pITG	✓	-	-
S2	L	aITG	-	-	-
S5	L	pITG	✓	-	-
S5	L	pITG	✓	-	-
S6	L	pITG	-	-	-
S8	R	pITG	✓	✓	-
S8	R	pITG	✓	-	-
S9	R	pITG	-	-	-

Hemi, hemisphere; Numeral active (relative to baseline); Numeral selective (relative to baseline, Latin letters, and foreign letters). (✓) Statistically significant at $P < 0.05$, FDR corrected.

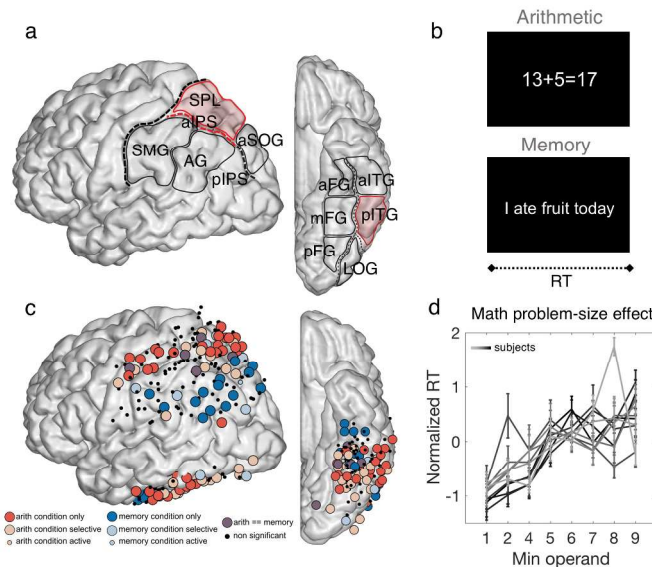


Figure 1. Anatomical subdivisions, task, recording sites, and behavioral problem-size effect.

A) The anatomical subdivisions within the lateral parietal cortex (LPC) and ventral temporal cortex (VTC) considered in this study, as seen in the left hemisphere from a slightly posterior viewpoint. LPC: AG, angular gyrus; aIPS, anterior intraparietal sulcus; aSOG, anterior superior occipital gyrus; pIPS posterior intraparietal sulcus; SMG, supramarginal gyrus; SPL, superior parietal lobule. VTC: aFG, anterior fusiform gyrus; aITG, anterior inferior temporal gyrus; pFG, posterior fusiform gyrus; mFG, mid fusiform gyrus; pITG, posterior inferior temporal gyrus. Arithmetic-ROIs marked in red. B) Exemplar stimuli of the Memory & Arithmetic verification task. In each trial, subjects were asked to verify the correctness of visually presented additions or a memory statements, by pressing one of two buttons. C) LPC and VTC sites from all 10 subjects are projected onto a single left hemisphere using the MNI space (see Electrodes Localization in the Methods), with the color of each site indicating its selectivity for arithmetic versus memory. Bright blue and bright red mark the most selective sites, passing three criteria for significance (e.g. arithmetic > baseline; arithmetic > memory; and memory indistinguishable from baseline). Faded red and blue indicate the selective sites that met only the first two criteria. Small faded red and blue indicate sites that met only the first criteria. Sites colored in purple were activated similarly during the two conditions, and sites marked by small black dots were not significantly active during either condition. Significance was defined as $P < 0.05$, FDR corrected within subject. D) Behavioral problem-size effect (min operand) in each subject (different shades of gray): average RT plotted as a function of min operand (normalized within each subject by subtracting the mean and dividing by the standard deviation).

254x190mm (290 x 290 DPI)

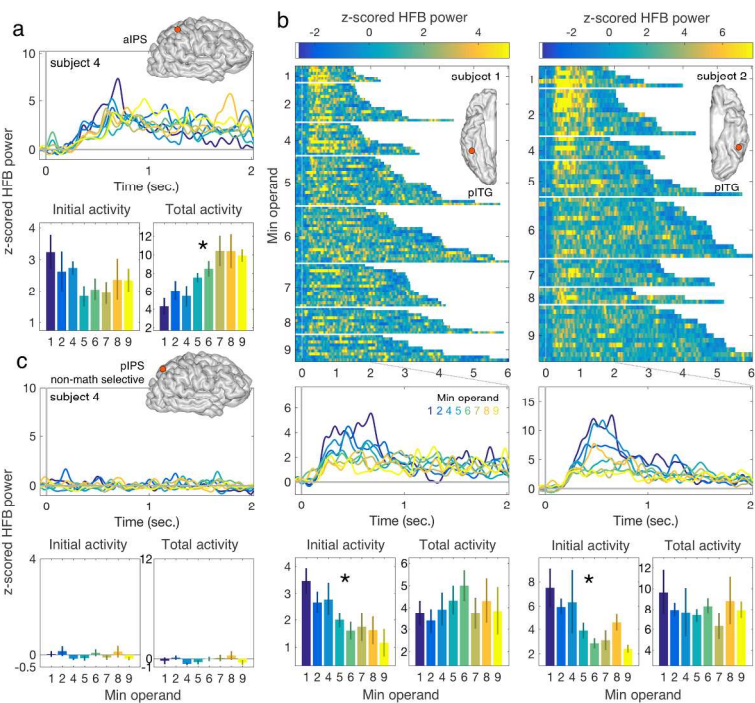


Figure 2. Example sites whose activity is modulated by the min operand.

A) Exemplar arithmetic selective channel in the aIPS showing increased HFB total activity as a function of min operand. The time course shows the activity averaged across trials with a given min operand (zoomed in the first two seconds of the trial). Bar plots show average initial activity (within the first second of a trial), and average total activity (integrated over the whole trial) as a function of min operand. B) Two exemplar channels showing decreased HFB initial activity in the pITG as a function of min operand (both arithmetic selective, one in each hemisphere in two different subjects). The first plot in each column shows the time course of activity for each trial, sorted by min operand and then by RT. C) Exemplar channel of a non-arithmetic selective channel in the posterior IPS of the same subject as in B showing no HFB modulation by min operand. An asterisk indicates that a regression analysis found a significant effect of min operand on either initial or total HFB activity ($P < 0.05$, FDR corrected).

254x190mm (290 x 290 DPI)

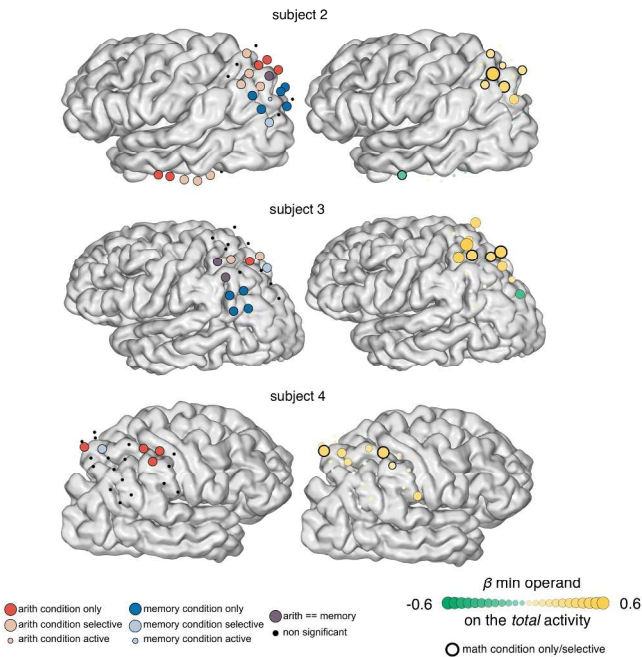


Figure 3. Anatomical and functional specificity of the HFB activity modulation in the LPC.

The figure illustrates the relationship, in LPC, between (1) selectivity for arithmetic vs. memory (left brain, same color code as Figure 1B) and (2) the effect of the min operand on total activity (right brain). The figure shows all 3 (out of 7) subjects with LPC coverage who showed the effect. Most channels whose total activity increased with problem size were located within the aIPS and SPL and were arithmetic selective, but some channels that showed this effect felt outside aIPS and SPL and/or were not arithmetic selective. For the min effect, dot color indicates the size and sign of the regression coefficient and dot size indicates the size of the regression coefficient. A thick black ring indicate that the channel is also arithmetic selective. Small dots indicate non-significant channels. P-values were FDR-corrected within subject.

254x190mm (290 x 290 DPI)

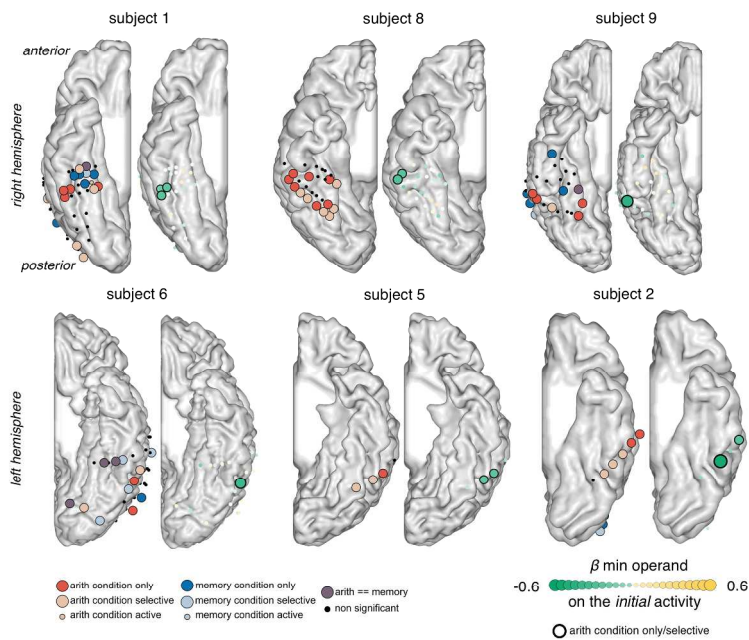


Figure 4. Anatomical and functional specificity of the HFB activity modulation in the VTC.

The figure illustrates the relationship, in VTC, between (1) selectivity for arithmetic vs. memory (left brain, same color code as Figure 1b) and (2) the effect of the min operand on initial activity (right brain). The figure shows all 6 (out of 7) subjects with pITG coverage who showed the effect. All channels whose initial activity decreased with problem size were located within the pITG (except for the most anterior channel of subject 2 - anterior ITG - and were arithmetic selective (thick black ring). For the min effect, dot color indicates the size and sign of the regression coefficient and dot size indicates the size of the regression coefficient (standardized) ($P < 0.05$, FDR corrected). Small dots indicate non-significant channels.

254x190mm (290 x 290 DPI)

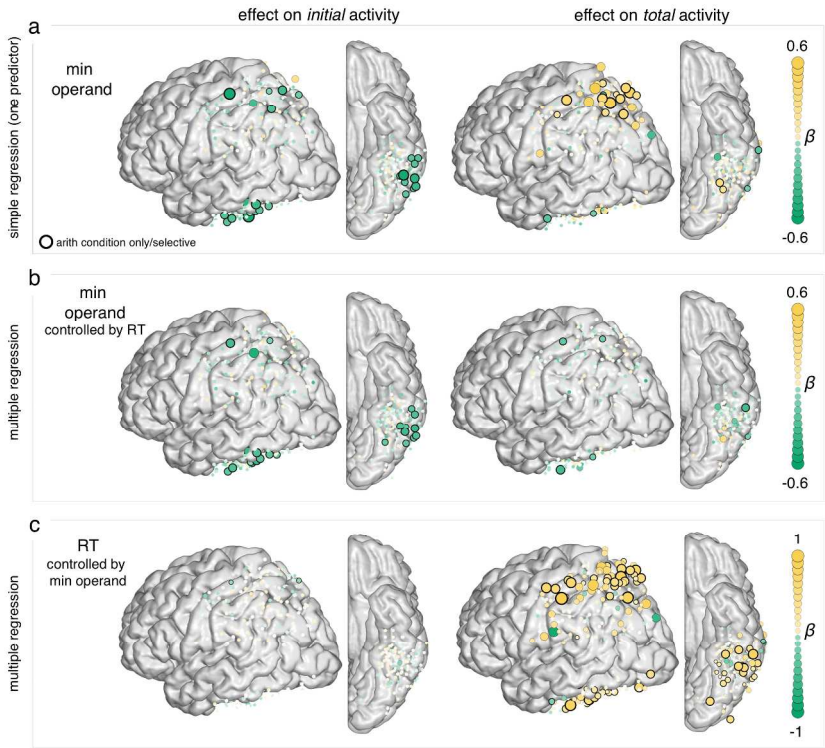


Figure 5. Modulation by min operand and RT in the LPC and VTC.

Regression analysis, where activity is modeled as a function of min operand in the initial activity (within the first second of a trial, left column) and total activity (integrated over the whole trial, right column). A) The effect of the min operand in a simple regression (one predictor). B) The effect of the min operand in a multiple regression that included both the min operand and the RT as predictors. C) The effect of the RT in a multiple regression that included both the min operand and the RT as predictors. For all plots, dot color indicates the size and sign of the regression coefficient and dot size indicates the size of the regression coefficient significant (standardized). A thick black ring indicate that the channel is also arithmetic selective. Small dots indicate non-significant channels. Significance: $P < 0.05$, FDR corrected.

254x190mm (290 x 290 DPI)